Population Inversion in a Single InGaAs Quantum Dot Using the Method of Adiabatic Rapid Passage

Yanwen Wu,[1] I. M. Piper,[1] M. Ediger,[1] P. Brereton,[1] E. R. Schmidgall,[1] P. R. Eastham,[2] M. Hugues,[3] M. Hopkinson,[3] and R. T. Phillips[1]

[1]*Cavendish Laboratory, University of Cambridge, J.J. Thomson Avenue, Cambridge CB3 0HE, United Kingdom*
[2]*School of Physics, Trinity College, Dublin 2, Ireland*
[3]*Department of Electronic and Electrical Engineering, University of Sheffield, Mappin Street, Sheffield S1 3JD, United Kingdom*

(Received 23 July 2010; revised manuscript received 22 November 2010; published 8 February 2011)

Preparation of a specific quantum state is a required step for a variety of proposed quantum applications. We report an experimental demonstration of optical quantum state inversion in a single semiconductor quantum dot using adiabatic rapid passage. This method is insensitive to variation in the optical coupling in contrast with earlier work based on Rabi oscillations. We show that when the pulse power exceeds a threshold for inversion, the final state is independent of power. This provides a new tool for preparing quantum states in semiconductor dots and has a wide range of potential uses.

DOI: 10.1103/PhysRevLett.106.067401 PACS numbers: 78.67.Hc, 42.50.Ct, 78.20.Ek

Preparation of a specific quantum state in a semiconductor quantum system is a required step for quantum computation [1,2], generation of single photons [3] and entangled photon pairs [4], and studies of Bose-Einstein condensation [5]. A two-level quantum system, such as that of an exciton in a single quantum dot, can be driven into a specified state by use of a coherent interaction between the system and a tuned optical field. Previously, the interaction used to invert a two-level system in semiconductor quantum dots has driven the system with a resonant transform-limited light field. In this case, in the Bloch sphere representation the Bloch vector precesses about a field vector which lies in the equatorial plane, and so the optical pulse rotates the Bloch vector from its initial position at the south pole (ground state) through an angle $\theta = \pi$ to the north pole (inversion). The angle $\theta = \int \frac{(\mu E)}{\hbar} dt$ is defined as the pulse area in a Rabi rotation where μ is the dipole moment describing the two-level system and $E(t)$ is the envelope of the optical field. Coherent resonant interaction has been shown to be capable of generating several such Rabi cycles, and permits readout of the state of the system optically [6–8], or electrically [9]. The Rabi approach requires precise control over the integrated pulse area (θ) to achieve an inversion angle of π as shown schematically in Fig. 1(a).

Here we show experimentally that state preparation is also possible by adiabatic rapid passage (ARP), which has the advantage that it is largely unaffected by variation in the dipole coupling, which is a normal feature of dot systems, and likewise insensitive to variation in the optical field which typically arises from laser fluctuation or positional variation in arrays of dots [10]. Several theoretical proposals have recognized the potential of ARP excitation to create entanglement between locally separated electron spins for robust two-qubit quantum operations [11,12], exert quantum control between two-subband quantum wells [13,14], and generate novel Bose-Einstein condensates in semiconductors [5]. ARP is a form of coherent interaction which effectively produces an anticrossing of the two quantum levels involved [15]. At an anticrossing the wave function weight associated with a particular energy eigenvalue always switches from one

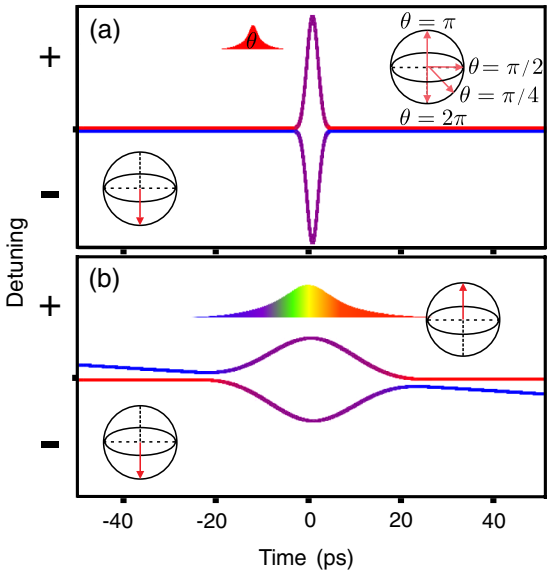

FIG. 1 (color online). Schematic representation of the eigenenergies of the two-level quantum system in the rotating frame of the optical field in the (a) Rabi excitation regime with a transform-limited 2 ps pulse and (b) the ARP regime with a chirped pulse of 15 ps pulse width. The red (blue) color represent the pure ground (excited) state of the system and the purple color represents the mixing of the two states during the pulse. For a system initially in the ground state, the Bloch spheres show that the final state of the system depends on the pulse area, θ, of the interacting field in (a), whereas in (b) the final inversion of the system is independent of the pulse energy.

state to the other as the anticrossing is traversed, and ARP uses this to switch the system from the ground state to the excited state as shown in Fig. 1(b).

For ARP to operate, the quantum dynamics during the interaction with the field must not be interrupted by random events leading to dephasing of the coherent superposition of the ground and excited states [16–18]. The quantization of electronic states in a semiconductor quantum dot leads to an electronic level structure discrete in energy. Cross-gap electronic excitation is primarily excitonic in character and scattering mechanisms characteristic of higher dimensional semiconductor structures are suppressed due to the quantum confinement potential of the dot. The ARP approach can be designed to invert a quantum system of multiple to excitons to a specific final state when a suitable optical pulse is constructed [10,19].

In order to detect the quantum state in which the system is left by the ARP interaction we have adopted the approach introduced by Zrenner *et al.* [9], who recognized that it is possible to read out a quantum state electronically. In the ground state, $|0\rangle$, there is no exciton, but the excited state, $|X\rangle$, corresponds to an electron in the conduction band and a hole in the valence band, bound by the mutual Coulomb interaction as an exciton. The resonant optical excitation takes the system from the ground state to an arbitrary coherent superposition with the upper state: $c_0|0\rangle + c_X|X\rangle$. The dot is embedded in a biased Schottky diode structure (Fig. 2), and the applied electric field leads to ionization of the excited state on a time scale longer on average than the excitation time. Clearly, the probability of charge flow depends on the relative amplitude in state $|X\rangle$; when the system is entirely inverted and $|c_X|^2 = 1$, the maximum possible current flow in the external circuit is one electron per excitation cycle in the case of perfect extraction. For a repetition of the incident laser pulse at a rate $f = 76$ MHz, the maximum current expected in this simple picture is just ef where e is the electron charge; here $ef = 12.2$ pA.

We have selected a single InGaAs dot formed by Stranski-Krastanow growth, observed through a 200 nm diameter aperture fabricated in a Ti/Au Schottky contact by electron-beam lithography, as illustrated schematically in Fig. 2(a). Within the structure the dot layer is separated from the heavily n-doped back layer by 40 nm of GaAs which acts as a tunneling barrier. The position of the dots with respect to the Fermi level can be changed by varying the bias applied to the top Schottky contact. Optical excitation and photoluminescence (PL) signal collection are achieved with a confocal microscopy setup. Illumination is at a photon energy higher than the gap for excitation of PL or by pulses from a mode-locked Ti:sapphire laser for the resonant pulse experiments. The pulses used for the Rabi and ARP excitations are a transform-limited hyperbolic secant pulse of 2 ps full width at half maximum (FWHM) and the same pulse chirped to give 15 ps

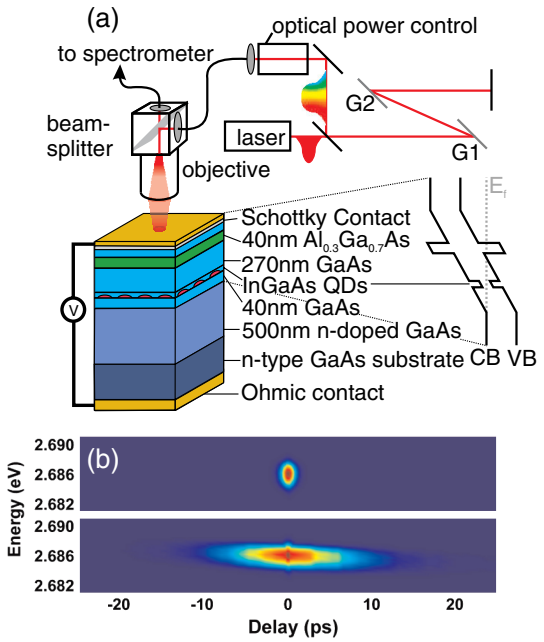

FIG. 2 (color online). (a) Schematic diagram of the sample structure and experimental setup. The linear chirp on the optical pulses is generated by a parallel grating pair with 1200 grooves/mm. The value of the chirp can be changed by varying the distance between the gratings. The laser light is focused by the objective down to ~ 1 μm over a 200 nm aperture in a gold mask. The sample consists of a single layer of InGaAs quantum dots embedded in a Schottky diode structure. The band diagram of the diode shows the relative positions of each layer in the growth direction and in energy. (b) A spectrally resolved autocorrelation scan (top) of a transform-limited pulse 2 ps FWHM and the cross correlation (bottom) of the same pulse chirped to give 15 ps FWHM.

FWHM, respectively. The characterizations of the pulses shown in Fig. 2(b) are spectrally and temporally resolved auto- and cross correlation signals from a frequency doubling crystal. The selection of the laser wavelength for the pulsed experiments is made by first conducting photoluminescence mapping of the transitions corresponding to this dot, as shown in Fig. 3(a).

Note that the dot can be switched from the negatively-charged exciton (X^-, $\sim$1.338 eV) to the neutral exciton (X, $\sim$1.3435 eV) and to the positively-charged exciton (X^+, $\sim$1.3445 eV) by varying the bias on the device, demonstrating the charge injection by tunneling [20]. Also present is neutral biexciton state (BX) which is emitted at about 1.341 eV corresponding to a binding energy of 3 meV. In order to read the quantum state of the dot by means of the ionization current the bias has to be chosen to suppress photoluminescence as the main recombination channel. We have chosen to operate the device at a bias of -1 V, which suppresses the PL signal but does not produce too short a tunneling time [21]. Figure 3(b) shows the photocurrent at that bias as a function of tunable

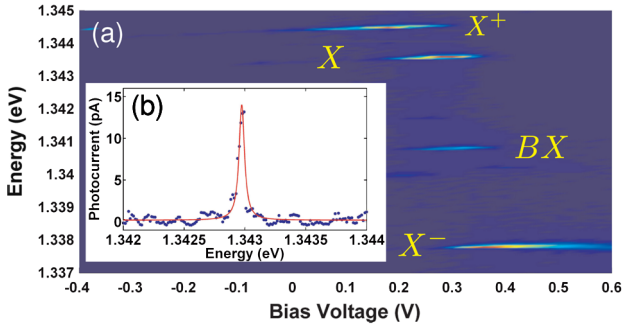

FIG. 3 (color online). (a) A PL map of the emission from various excitonic states at different bias voltages. X^+ is the positively charged exciton, X is the neutral exciton, BX is the neutral biexciton, and X^- is the negatively-charged exciton. (b) Photocurrent versus the wavelength of a continuous-wave excitation laser at -1 V bias voltage. The FWHM of the line shape is 50 μeV.

continuous-wave laser wavelength incident on the structure; the photocurrent peak at 1.343 eV corresponds to resonant excitation of X, with the transition energy modified slightly by the applied field. The width of the photocurrent resonance is indistinguishable from the linewidth of the cw Ti:sapphire laser used to excite the dot. The tunneling time is therefore much longer than the time deduced from the measured linewidth, which itself corresponds to a limiting value of 25 ps. We estimate that any change in linewidth associated with the tunneling must correspond to a time at least an order of magnitude longer than this. Therefore, we believe that the tunneling takes place on a time scale much longer than the duration of the chirped pulses used here to produce ARP.

Under pulsed excitation with a 2 ps transform-limited hyperbolic secant pulse with zero temporal chirp ($\alpha = 0$ ps^{-2}; see definition below), tuned to coincide with the photocurrent peak, the system clearly exhibits Rabi oscillation as the pulse area (proportional to [incident power]$^{(1/2)}$) is increased, as shown in Fig. 4(a) by the solid circle symbols. The first peak of the Rabi flop corresponds to the exciton being left in the excited state after the pulse has passed (Bloch vector toward the north pole), whereas the first trough corresponds to a Rabi rotation through the exciton and back to the ground state (Bloch vector toward the south pole). The data in Fig. 4(a) represent the difference between the current drawn when the spectrum of the pulse overlaps the transition and when it is detuned from it. The presence of a linear background current has been reported in previous work on electrical readout of this form [9,17], and is associated with weak absorption processes anywhere within the depletion region of the device. When the same optical pulse is chirped by the grating pair [$G1$ and $G2$ in Fig. 2(a)] to give a temporal chirp of $\alpha = 0.089$ ps^{-2}, and a chirped pulse width of 15 ps FWHM, the result is a clear signature of ARP, as shown in Fig. 4(a) by the open square

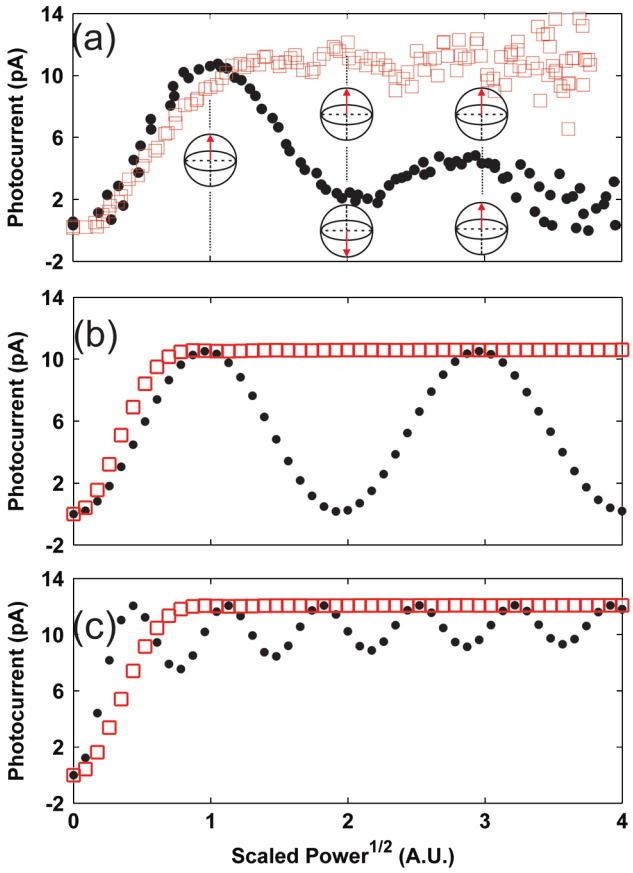

FIG. 4 (color online). (a) Electrical readout signals of Rabi oscillation (solid circles) excited by the 2 ps transform-limited pulse and ARP (open squares) excited by the 15 ps chirped pulse. The curves are the difference between the on-resonant (1.343 eV) photocurrent and the corresponding off-resonant (1.341 eV) background photocurrent. The small Bloch spheres indicate the position of the Bloch vector at given excitation powers in each case. (b) Simulation of the corresponding electrical readout signals in (a) using the same optical pulse characterization and dot properties as the experiment assuming a recombination time of 1 ns and tunneling T_2 of 300 ps. (c) Simulation of electrical readout signals using recombination time of 1 ns, tunneling T_2 of 25 ps and a 15 ps transform-limited (chirped) pulse for the Rabi (ARP) simulation.

symbols, where the current rises initially as the pulse power is increased, and then stabilizes at a value corresponding to inversion, with no further change as the pulse area is increased. Thus at an equivalent pulse power to that which left the system back in the ground state, with ARP the dot is left inverted. The bandwidth of the pulses used here is 0.3 meV, which is much smaller than the binding energy of the biexciton. Therefore contribution from the biexciton transition is negligible.

We can compare the measured readout of the quantum state of the system with a calculation of the current using the methods described by Villas-Bôas *et al.* [18], and Schmidgall *et al.* [10]. This system can be described by the Hamiltonian

$$H = E_X|X\rangle\langle X| - \frac{\mu_X}{2}(E(t)|0\rangle\langle X| + E^*(t)|X\rangle\langle 0|). \quad (1)$$

The dipole coupling is specified by μ_X and the optical field by $E(t)$. Under a unitary transformation

$$U(t) = \exp[0|0\rangle\langle 0| + i\omega(t)t|X\rangle\langle X|] \quad (2)$$

yields a picture appropriate to interaction driven by an applied field whose frequency varies in time as $\omega(t)$. The simplest variation is linear in time, with $\omega(t) = \omega_0 + \frac{\alpha t}{2}$, where α is the linear temporal chirp. This is the form of optical field produced by the grating pair. The Hamiltonian in the rotating frame of the central optical field frequency, ω_0, is

$$H_{\text{eff}} = \begin{pmatrix} 0 & -\frac{1}{2}\mu_X E_0(t) \\ -\frac{1}{2}\mu_X E_0(t) & \Delta_X - 2\hbar\dot{\omega}(t) \end{pmatrix}, \quad (3)$$

where the detuning of ω_0 from the transition frequency of the exciton is Δ_X. In the experiment, Δ_X is zero. In this picture, the condition for adiabatic transfer [15,22] is that the effective Rabi frequency $\Omega(t) = \sqrt{|\Omega_0(t)|^2 + \delta(t)^2}$ satisfies $\frac{\dot{\Omega}_0}{\Omega^2} \ll 1$, and $\frac{\dot{\delta}}{\Omega^2} \ll 1$, where $\hbar\delta = \Delta_X - \hbar\dot{\omega}t$ and $\Omega_0(t) = \mu_X E_0(t)/\hbar$. In other words, the rates of change in the frequency and field amplitude of the optical pulse are both slow in comparison to the effective Rabi frequency. In this adiabatic regime, the Bloch vector follows the field vector as it rotates at a rate of $\dot{\delta}$ from one polar extreme to another during the pulse while precessing rapidly at a rate Ω around the field vector within a small solid angle.

To calculate the current drawn from the dot in the presence of both dephasing and ionization of the exciton, the Hamiltonian model of the individual system is used to evaluate the time evolution of the density matrix; the current is calculated from the scattering term corresponding to taking state $|X\rangle$ to state $|0\rangle$ by ionization, using the Lindblad form [23] of the scattering terms as described by Schmidgall *et al.* [10]. This term is integrated throughout the pulse interaction. Note that this model does not incorporate terms intended to explain the reduction in contrast of the Rabi oscillation usually observed for high values of pulse area in Rabi flopping [16–18,24–26]. For realistic values of dephasing and tunneling parameters, the model generates the curves shown in Fig. 4(b), which confirm that the measured signals correspond to ARP. Simulations in Fig. 4(c) further show the results of Rabi and ARP excitations using unchirped and chirp pulses of the same temporal width (15 ps) with a tunneling time of 25 ps, which confirms that the signature of ARP would be clear in the experiment we have conducted even if the tunneling time approached within a factor of 2 of the chirped pulse duration.

Our results demonstrate the possibility of quantum state inversion in a system measured by electrical readout, robust with respect to variation in the details of the strength of the optical interaction. This opens the possibility of using ARP in a range of contexts, including inversion of systems with level structures which can lead to deterministic single photon emission, or entangled photon pair emission, and two-spin gate via trions [12]. The insensitivity to the details of the interaction can be expected to provide access for the first time to physics associated with injection of tailored inversion profiles, such as complex microcavity electrodynamics.

This work is supported by EPSRC grant EP/F040075/1. Y. W. is grateful for a Herchel Smith Fellowship. P. R. E. is supported by the Science Foundation Ireland grant SFI/SIRG/I1592. We thank Professor Dr. Artur Zrenner for his advice on the fabrication of a Schottky device with low leakage current for electrical readout, and Dr. Geb Jones and Jonathan Griffiths for invaluable assistance with electron-beam lithography.

[1] D. P. DiVincenzo, Science **270**, 255 (1995).
[2] E. Farhi *et al.*, Science **292**, 472 (2001).
[3] P. Michler *et al.*, Science **290**, 2282 (2000).
[4] R. M. Stevenson *et al.*, Nature (London) **439**, 179 (2006).
[5] P. R. Eastham and R. T. Phillips, Phys. Rev. B **79**, 165303 (2009).
[6] T. H. Stievater *et al.*, Phys. Rev. Lett. **87**, 133603 (2001).
[7] H. Kamada, H. Gotoh, J. Temmyo, T. Takagahara, and H. Ando, Phys. Rev. Lett. **87**, 246401 (2001).
[8] H. Htoon *et al.*, Phys. Rev. Lett. **88**, 087401 (2002).
[9] A. Zrenner *et al.*, Nature (London) **418**, 612 (2002).
[10] E. R. Schmidgall, P. R. Eastham, and R. T. Phillips, Phys. Rev. B **81**, 195306 (2010).
[11] U. Hohenester, J. Fabian, and F. Troiani, Opt. Commun. **264**, 426 (2006).
[12] S. K. Saikin, C. Emary, D. G. Steel, and L. J. Sham, Phys. Rev. B **78**, 235314 (2008).
[13] A. A. Batista and D. S. Citrin, Phys. Rev. B **74**, 195318 (2006).
[14] A. A. Batista, Phys. Rev. B **73**, 075305 (2006).
[15] V. S. Malinovsky and J. L. Krause, Eur. Phys. J. D **14**, 147 (2001).
[16] J. M. Villas-Bôas, S. E. Ulloa, and A. O. Govorov, Phys. Rev. Lett. **94**, 057404 (2005).
[17] A. J. Ramsay *et al.*, Phys. Rev. Lett. **104**, 017402 (2010).
[18] J. M. Villas-Bôas, S. E. Ulloa, and A. O. Govorov, Solid State Commun. **134**, 33 (2005).
[19] H. Y. Hui and R. B. Liu, Phys. Rev. B **78**, 155315 (2008).
[20] M. Ediger *et al.*, Appl. Phys. Lett. **86**, 211909 (2005).
[21] F. Findeis, M. Baier, E. Beham, A. Zrenner, and G. Abstreiter, Appl. Phys. Lett. **78**, 2958 (2001).
[22] S. A. Malinovskaya, Opt. Commun. **282**, 3527 (2009).
[23] G. Lindblad, Commun. Math. Phys. **48**, 119 (1976).
[24] H. S. Brandi, A. Latgé, Z. Barticevic, and L. E. Oliveira, Solid State Commun. **135**, 386 (2005).
[25] A. Vagov, M. D. Croitoru, V. M. Axt, T. Kuhn, and F. M. Peeters, Phys. Rev. Lett. **98**, 227403 (2007).
[26] Q. Q. Wang *et al.*, Phys. Rev. B **72**, 035306 (2005).